Regular and irregular vibrational states: Localized anharmonic modes and transition-state spectroscopy of Na 3

Nicholas J. Wright and Jeremy M. Hutson

Citation: The Journal of Chemical Physics **112**, 3214 (2000); doi: 10.1063/1.480905
View online: http://dx.doi.org/10.1063/1.480905
View Table of Contents: http://scitation.aip.org/content/aip/journal/jcp/112/7?ver=pdfcov
Published by the AIP Publishing

Regular and irregular vibrational states: Localized anharmonic modes and transition-state spectroscopy of Na_3

Nicholas J. Wright[a] and Jeremy M. Hutson[b]
Department of Chemistry, University of Durham, South Road, Durham, DH1 3LE, United Kingdom

(Received 10 November 1999; accepted 24 November 1999)

We have calculated the lowest 900 vibrational energy levels and wave functions for the quartet ($1^4A_2'$) state of Na_3. The equilibrium geometry of the trimer is triangular, but the calculations include many states that lie above the barrier to linearity. Most of the high-lying states are irregular, but there are a few relatively localized states embedded in the irregular bath. The localized modes observed include a ''horseshoe'' mode and a symmetric stretch centered on the linear transition state. The density of states and couplings are such that in most cases the ''horseshoe'' character is spread over several bath states, while the symmetric stretch states exist in a purer form. The localized states could be observed in laser-induced fluorescence, stimulated-emission pumping or ion photodetachment spectroscopy from a state with a linear equilibrium geometry. © *2000 American Institute of Physics.* [S0021-9606(00)00807-2]

I. INTRODUCTION

The vibrational energy levels of polyatomic molecules govern many important chemical processes. The wave functions and level distribution reflect the underlying structure of the phase space for the molecule. Because of the chaotic nature of the phase space at high energies, the high-lying vibrational states might be expected to be irregular. It has been found in several studies, however, that this is far from the case: Some states in the ''classically chaotic'' region are strongly localized, with wave functions that exhibit regular nodal patterns and do not sample all of the available phase space. Previous studies on H_3^+,[1–6] LiCN,[7] KCN[8] and Ar_3[9–11] have identified several different localization features, which have been termed ''localized anharmonic modes.''[11]

Prominent amongst the localization features observed in H_3^+ and Ar_3 are the so-called ''horseshoe'' states. These correspond to a motion in which the molecule passes from one equilateral triangle geometry to another equivalent one: one atom moves between the other two, with the two outer atoms moving apart to make way for it. Classical calculations by Gomez Llorente, and Pollak[12] suggested that these states were responsible for the coarse-grained features in the H_3^+ photofragmentation spectra of Carrington and Kennedy.[13] Further studies by Le Sueur, Henderson, and Tennyson showed that horseshoe states corresponded to intensity peaks in the calculated spectra for excitation from the ground state.[4] In calculations on Ar_3, the regular nodal patterns of the horseshoe states were clearly visible in the wave functions,[9–11] and it was also possible to identify a ''linear symmetric stretch mode,'' where the wave function amplitude was concentrated about the linear transition-state configuration.[11] For Ar_3,[14] as for H_3^+,[15,2,5] the regular nodal patterns were shown to be localized around the trajectories of stable periodic orbits.

Highly excited states of Ar_3 may be difficult to observe. However, there are other systems that are more amenable to experiment. For example, Higgins *et al.*[16] have recently observed laser-induced fluorescence spectra of quartet states of Na_3 on the surface of helium droplets. They excite from the lowest quartet state ($1^4A_2'$), which is bound principally by van der Waals forces, to the $2^4E'$ state. When the zero-point level of the $2^4E'$ state is excited, the resulting fluorescence spectra probe levels of the lowest quartet state with up to 350 cm^{-1} of vibrational energy. The $2^4E'$ state has a nonequilateral geometry because of the Jahn–Teller effect. *Ab initio* potential energy surfaces have been computed and bound-state calculations performed to assign the transitions measured.[16,17] The calculated potential energy surface for the lowest quartet state is highly nonadditive.

The computational method used in Refs. 16 and 17 is suitable for low-lying states, but would be very difficult to converge for horseshoe states. The purpose of the present work is to carry out calculations on the higher-lying states, to assess the role of localized anharmonic modes and suggest how they could be observed.

II. THEORY

The theoretical methods used in this work are identical to those used in Ref. 11. A more detailed description can be found there.

We use a Jacobi coordinate system to represent a triatomic system ABC as an atom A interacting with a diatom BC. The vector **r** of length *r* runs from atom B to atom C

[a]Present address: Department of Physical Chemistry and The Fritz Haber Research Center, The Hebrew University, Jerusalem 91904, Israel and Department of Chemistry, University of California, Irvine, California 92697.
[b]Electronic mail: J.M.Hutson@durham.ac.uk

(where atom B is the heavier of B and C if they are different). The vector **R** of length R runs from the center of mass of BC to atom A. θ is the angle between **r** and **R**.We use a discrete variable representation (DVR)[18,19] to describe the wave functions. The DVR is advantageous because it allows the grid of basis functions to be tailored to the region of interest. In addition, the DVR Hamiltonian matrix is very sparse, so that it can be diagonalized efficiently using an iterative diagonalizer. In the notation of Choi and Light,[20] the DVR Hamiltonian matrix elements are

$$\begin{aligned}\mathbf{H}^{\alpha'\beta'\gamma'K'}_{\alpha\beta\gamma K} &= \sum_{ii'jj'll'} {}^{R}T_{i'\alpha'}{}^{r}T_{j'\beta'}{}^{K\theta}T_{l'\gamma'}H^{i'j'l'K'R}_{ijlK}T_{i\alpha}{}^{r}T_{j\beta}{}^{K\theta}T_{l\gamma} \\ &= {}^{R}d_{\alpha'\alpha}\delta_{\beta'\beta}\delta_{\gamma\gamma'}\delta_{K'K} + {}^{r}d_{\beta'\beta}\delta_{\alpha'\alpha}\delta_{\gamma\gamma'}\delta_{K'K} + \frac{\hbar^2}{2}\left(\frac{1}{\mu_1 R_\alpha^2}+\frac{1}{\mu_2 r_\beta^2}\right)^{\theta K} d_{\gamma'\gamma}\delta_{\alpha'\alpha}\delta_{\beta\beta'}\delta_{K'K} \\ &+ \frac{\hbar^2}{2\mu R_\alpha^2}([J(J+1)-2K^2]\delta_{\alpha'\alpha}\delta_{\beta'\beta}\delta_{\gamma\gamma'}\delta_{K'K} - [1+\delta_{K0}]^{1/2}\Lambda^{+}_{JK}B^{+}_{\gamma\gamma'K}\delta_{\alpha'\alpha}\delta_{\beta'\beta}\delta_{K'K+1} \\ &- [1+\delta_{K'0}]^{1/2}\Lambda^{-}_{JK}B^{-}_{\gamma\gamma'K}\delta_{\alpha'\alpha}\delta_{\beta'\beta}\delta_{K'K-1}) + V^{\alpha'\beta'\gamma'}_{\alpha\beta\gamma}\delta_{K'K}. \end{aligned} \quad (1)$$

The first two terms are the kinetic energy operators associated with the two radial coordinates, R and r, the third term is the angular kinetic energy, the fourth term contains the centrifugal term and the Coriolis coupling, and the final term is the potential energy. The transformation matrices T are labeled by superscripts R, r, and $K\theta$ to indicate the coordinate that they refer to. Greek suffixes refer to DVR points and Roman suffixes to functions in the corresponding finite basis representation. The reduced masses μ_1 and μ_2 correspond to the complete complex ($2M_{\mathrm{Na}}/3$ here) and the diatom ($M_{\mathrm{Na}}/2$ here), respectively. All calculations in the present work are for $J=0$, so that the centrifugal term and the Coriolis coupling are zero.

The nth wave function of the system, with parity p and total angular momentum J, may be expanded in the finite basis representation as

$$\Psi^{pJ}_n(R,r,\theta) = R^{-1}r^{-1}\sum_{ijlK} c^{Jp}_{ijlKn}\,\phi^R_i(R)\phi^r_j(r)P^K_l(\cos\theta), \quad (2)$$

where the functions $P^K_l(\cos\theta)$ are associated Legendre polynomials. The functions $\phi^R_i(R)$ and $\phi^r_j(r)$ are potential-optimized basis functions in R and r. These are obtained as solutions of one-dimensional (1D) Schrödinger equations with one-dimensional effective potentials for the motions in R and r. The effective potentials are constructed in the same way as in Ref. 11. From these 1D functions the DVR quadrature points are obtained using the method of Harris, Engerholm, and Gwinn (HEG).[21]

The molecular symmetry group of Na_3 is $D_{3h}(M)$. The only symmetry operation that appears naturally in Jacobi coordinates, however, is permutation of the labels of the ''diatom'' nuclei, which has the effect $\theta \rightarrow \pi - \theta$. Use of the Jacobi coordinate system effectively reduces the molecular symmetry group to $C_{2v}(M)$. The Hamiltonian matrix splits into two blocks, symmetric and antisymmetric with respect to the permutation. In terms of labels of $D_{3h}(M)$, the even block contains A_1 and E (component 1) and the odd block contains A_2 and E (component 2). The even symmetric block contains only functions with l even in Eq. (2) and the odd block contains only functions with l odd.

We obtain the eigenvalues and eigenvectors of the Hamiltonian matrix using the implicitly restarted Lanczos method (IRLM) as described by Sorensen.[22,23] The method does not require explicit construction of the Hamiltonian matrix; only matrix-vector products involving the Hamiltonian are needed. This allows diagonalization of matrices far larger than could be stored in computer memory. To improve the convergence rate of the IRLM scheme we use the Chebychev polynomial preconditioning scheme described by Korambath, Wu, and Hayes.[24]

III. POTENTIAL ENERGY SURFACE

In this work we use the potential of Higgins *et al.*[17] to describe the $1^4A_2'$ state of Na_3. This potential was obtained from a grid of coupled-cluster [CCSD(T)] calculations with a large basis set, interpolated using the reproducing-kernel Hilbert space scheme of Ho and Rabitz.[25] The potential has a global minimum at $-849.4\ \mathrm{cm}^{-1}$, with the atoms in an equilateral triangle configuration 4.41 Å apart. The barrier to linearity is at $-385.3\ \mathrm{cm}^{-1}$ ($464.1\ \mathrm{cm}^{-1}$ above the minimum), with $r=5.10$ Å. Comparison with the corresponding Na–Na pair potential,[26] which has $R_e=5.192$ Å and $D_e=177.7$

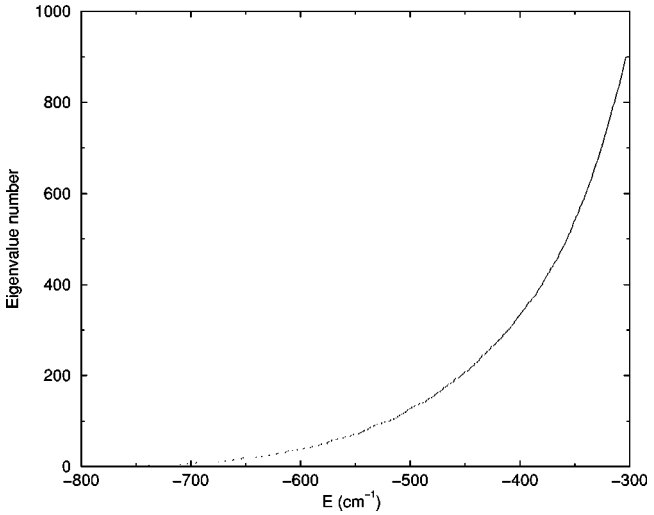

FIG. 1. The vibrational eigenvalue distribution for the $1^4A_2'$ state of Na_3. The density of states is the gradient of the curve.

cm^{-1}, shows that large nonadditive effects are present in Na_3 and that they are especially prominent at the equilibrium geometry.

The large nonadditive contribution to the Na_3 potential energy surface makes its shape qualitatively different from that for Ar_3, where the nonadditive effects are small and can, to a good first approximation, be neglected. The nonadditive forces significantly decrease the Na–Na distances at the equilibrium configuration when compared with both the dimer and the linear configuration.

IV. RESULTS AND DISCUSSION

We have calculated the lowest 900 $J=0$ energy levels and wave functions of Na_3 ($1^4A_2'$). The DVR basis set was constructed from 28 points in θ, 40 points in R and 38 points in r. The 40 points in R were obtained by integrating the 1D Schrödinger equation from 0 to 10 Å. The quadrature points in r were obtained similarly, propagating from $r=3$ to 12 Å.

Our present calculations are limited to the lowest 900 states by memory restrictions. However they provide one over 400 energy levels above the barrier to linearity, which is sufficient to examine the dynamics in this region. The difference between the energies of the corresponding E levels in the even and odd symmetry blocks can give a measure of the convergence of the calculation. For Na_3 such a comparison is only possible for the lowest 400 levels or so and indicates that our calculation is converged to approximately 0.5 cm^{-1} in this region (though much better near the bottom of the well). For higher levels the density of states is simply too great to be able to identify the corresponding components of E levels from the two symmetries. Although the calculation is not of spectroscopic accuracy above the barrier, we believe that the properties we are interested in, the localization features present in the wave functions, will not be significantly altered by increasing the convergence of the calculation.

The cumulative energy level distribution is shown in Fig. 1; the density of states is the gradient of this. A similar plot in Ar_3 shows a sharp increase near the barrier to linearity because a significant amount of extra phase space becomes available at that point.[11] In quartet Na_3, by contrast, no such sharp increase is present. In this system the much deeper well provides more phase space below the barrier, so that the extra encounted on reaching the barrier to linearity is less significant.

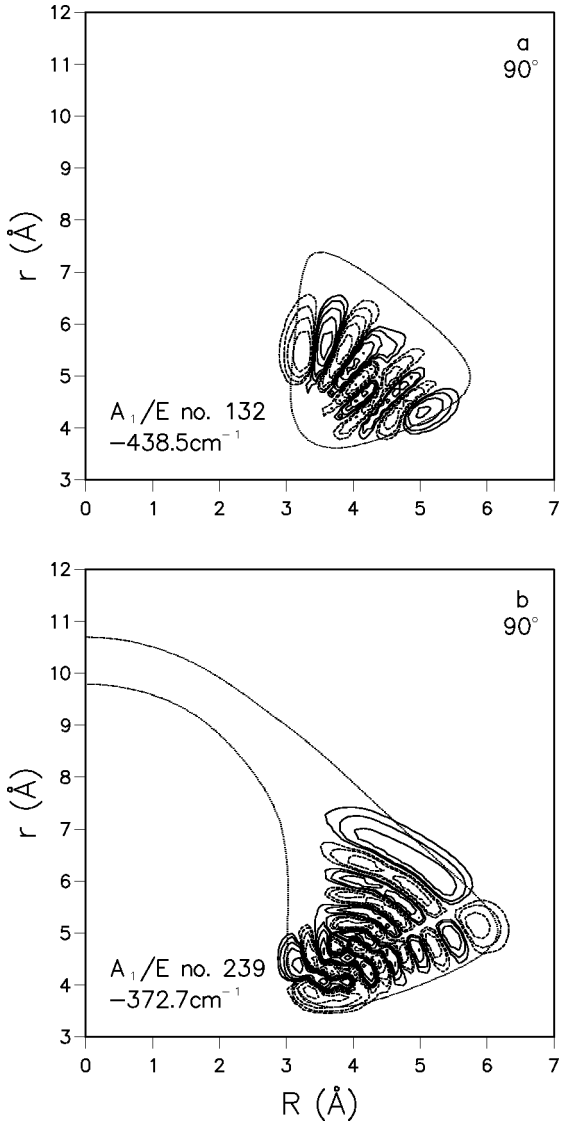

FIG. 2. Vibrational wave functions of quartet Na_3, plotted in Jacobi coordinates as a function of R and r for $\theta=90°$. The dotted line shows the boundary of the classically allowed region at the energy concerned. Solid and dashed contours show positive and negative values of the wave function. Contours are for 0.64, 0.32, 0.16, 0.08 and 0.04 of the maximum amplitude.

Selected vibrational wave functions for Na_3 are shown as contour plots in Figs. 2–4. Although the wave functions are functions of three coordinates, they are presented here as cuts at fixed θ as this provides the clearest representation for the present study.

It is possible to assign the lowest vibrational levels of quartet Na_3 in terms of the normal mode quantum numbers of a D_{3h} molecule. Such an assignment can be made from visual inspection of the wave functions up to approximately -480 cm^{-1} (~ 300 cm^{-1} above the ground state). Above

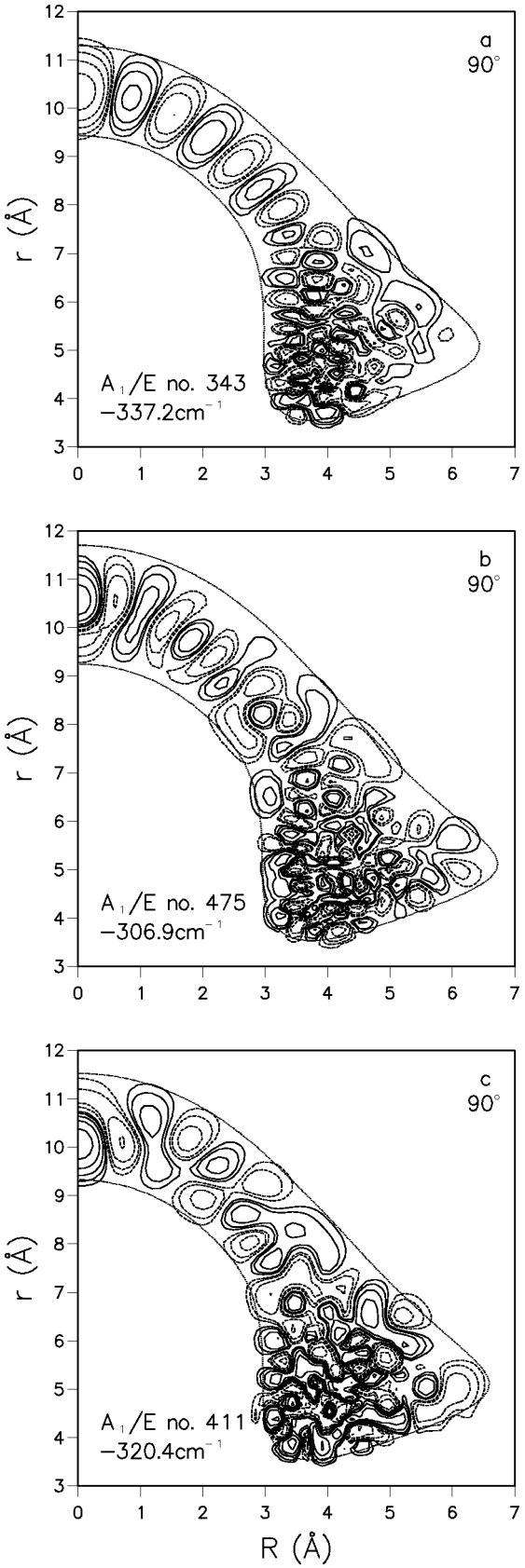

FIG. 3. Vibrational wave functions of quartet Na_3, plotted as in Fig. 2.

this energy the regular nodal patterns in the wave functions begin to disappear, making such an assignment impossible and to some extent meaningless. Even in this region, however, a few of the states remain assignable in terms of normal-mode quantum numbers. These are usually pure overtones or combinations with only 1 or 2 quanta of excitation in one of the modes. For example, A_1/E state number 131 is shown in Fig. 2(a) and is clearly a state with 9 quanta of excitation in the asymmetric stretch mode. This behavior persists up to the barrier to linearity; A_1/E state number 239, which has 10 quanta of excitation in the symmetric stretch mode and 1 in the asymmetric mode, is shown in Fig. 2(b) and is the last that is assignable in this way.

The horseshoe states previously observed in H_3^+ and Ar_3 are also present in Na_3. They are however present in a much less ''pure'' form. The larger barrier in Na_3 means that there are many more energy levels below the barrier than in Ar_3. At the barrier the density of states is already about 3 states per cm^{-1} in Na_3. This large density of states means that the localization features that are present above the barrier have many more ''bath'' states to couple to, so that their features are spread over many more eigenstates.

A complete assignment of all the horseshoe states based on inspection of their wave functions, which was achieved for both H_3^+ and Ar_3, is not possible for Na_3. The best example of a horseshoe state in Na_3 is shown in Fig. 3(a). The horseshoe features are clearly visible and, with careful counting, this state can be assigned as having 20 quanta of excitation. However it is far from typical. The state shown in Fig. 3(b) is much more representative. By comparison with the typical bath state shown in Fig. 3(c), it clearly has some horseshoe character. However the nodal structure for $r<7$ Å has no regularity; the nodal planes are no longer perpendicular to the path of the horseshoe motion and any quantum number assignment is fraught with uncertainty. This contrasts with Ar_3 and H_3^+, for both of which the horseshoe states show clear localization features across the whole range in r (and R).

The horseshoes are not the only regular states above the barrier. Indeed, the linear symmetric stretch states exist in a purer and more localized form than the horseshoes. Figure 4 shows states with quantum numbers $n_s=0-3$ in this mode. As in H_3^+ and Ar_3, states corresponding to combinations of the linear symmetric stretch mode and the horseshoe are also visible.

It is of great interest to consider how the localized anharmonic modes could be observed experimentally. Their characteristic feature is that they all show regular behavior around the barrier to linearity: they are in a real sense ''transition-state modes.'' In H_3^+, Le Sueur, Henderson, and Tennyson[4] showed that horseshoe states produced intensity peaks in spectra involving direct excitation from the triangular ground state. This may be true in quartet Na_3 as well, but the intensities are likely to be very low. A more promising approach is to access the transition-state modes from an excited electronic state, using laser-induced fluorescence or stimulated-emission pumping. The localization features might be visible in transitions from the $2^4E'$ state already observed, which has a nonequilateral geometry because of the Jahn–Teller effect. However, they would be most prominent in emission from a state with a linear or near-linear geometry. Alternatively, transition-state spectra could be observed by photodetachment from a state of the anion with a

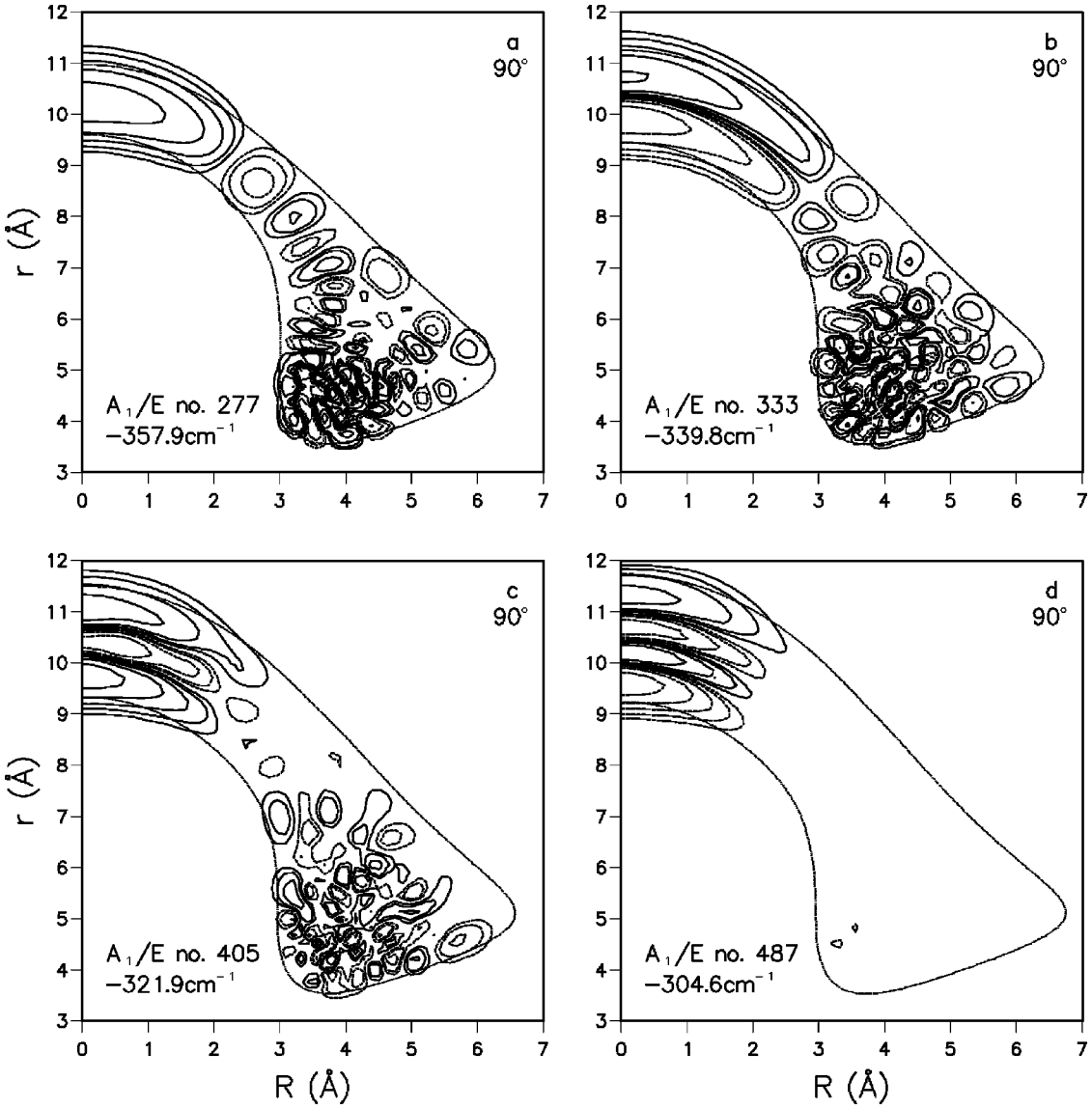

FIG. 4. Vibrational wave functions of quartet Na_3 for states involving excitation in the linear symmetric stretch mode, plotted as in Fig. 2. (a)–(d) States with $n_s=1-4$ quanta of stretch excitation.

linear equilibrium geometry. Unfortunately, not enough work has yet been done to establish whether such linear states exist for quartet Na_3 or triplet Na_3^-.

To investigate how the localized anharmonic modes would appear in transitions from a linear species, we have calculated the overlap between each vibrational wave function and a function localized at $R=0$ and $\theta=90°$, with a Gaussian profile in r (centered at $r=9.75$ Å with width 0.5 Å). The results are shown in Fig. 5, both as a stick spectrum and smoothed by convoluting with a Gaussian of width 0.4 cm^{-1}. The individual states give widely varying intensities, because the localized character is usually spread over several eigenstates. Nevertheless, the localized modes do give rise to fairly regular progressions in the low-resolution spectrum, and these might well be experimentally observable. With the aid of visual inspection of the wave functions, the peaks in the low-resolution spectrum can be assigned to progressions in the horseshoe mode for different excitations of the linear symmetric stretch as shown by the ''combs'' in Fig. 5.

Localization effects such as these will not be confined to quartet Na_3. They may be expected for any trimer with a triangular equilibrium geometry and an accessible linear transition state. Indeed, analogous localization features centered around transition-state geometries may be found for a much wider range of species and geometries.

V. CONCLUSIONS

We have calculated vibrational energy levels and wave functions for the lowest quartet ($1^4A_2'$) state of Na_3. The equilibrium structure of this species is triangular, but the calculations extend to states well above the barrier to linearity.

In quartet Na_3, as for H_3^+ and Ar_3, most of the states above the barrier are irregular in nature; they fill all the energetically available configuration space and their wave functions have no obvious nodal pattern. However there are regular states embedded in the bath of irregular states, analo-

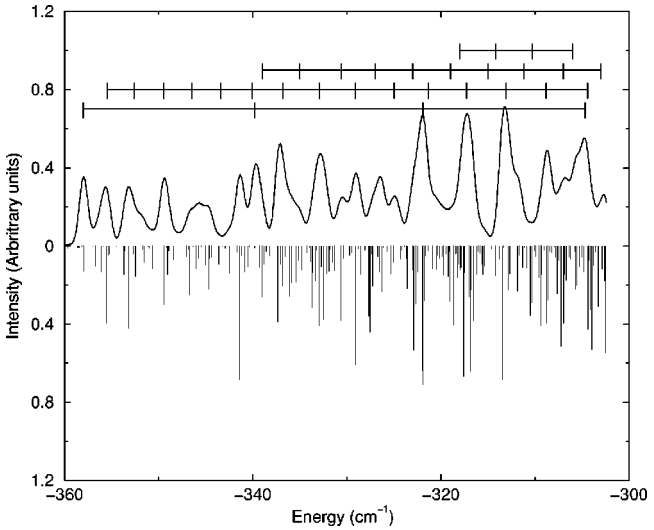

FIG. 5. Simulated spectra for a transition from Na_3 in a linear configuration to the quartet state. The peaks in the spectra correspond to the regular features observed in the wave functions. The combs on the plot indicate the positions of progressions of the regular features. From bottom to top they correspond to the linear symmetric stretch mode, the horseshoe mode, the horseshoe plus 1 quantum of linear symmetric stretch and the horseshoe plus 2 quanta of linear symmetric stretch.

gous to the ''horseshoe'' states previously identified for H_3^+ and Ar_3 and the ''linear symmetric stretch'' states of Ar_3. The character of these localized states is in most cases spread over several eigenstates, but the localization features nevertheless leave characteristic signatures in the spectrum.

Quartet Na_3 does show some differences from H_3^+ and Ar_3 because the barrier to linearity is much higher. The increased density of states makes it impossible to assign quantum numbers to the horseshoe states by visual inspection of the wave functions. The linear symmetric stretch states, however, remain relatively pure and can be assigned easily.

The effects of the localization features should be experimentally observable. The most promising experiments for quartet Na_3 are laser-induced fluorescence or stimulated-emission pumping, ideally from an excited quartet state with a linear equilibrium geometry, or photodetachment from a linear state of the triplet Na_3^- ion. Such a photodetachment scheme has already been implemented for doublet Ag_3,[27–29] although in that case the density of states at the energy of the barrier is very high. Other trimers, such as Li_3 and K_3, may be better candidates.

ACKNOWLEDGMENTS

N.J.W. thanks the Royal Society for a postdoctoral fellowship during which part of this work was carried out and EPSRC for funding in Durham. We would like to thank Giacinto Scoles for bringing this problem to our attention, Tak-San Ho for supplying his potential energy routine, and Benny Gerber for valuable discussions. The calculations were carried out on a Silicon Graphics Origin 2000 computer system, which was purchased with funding from the EPSRC. We are grateful to Dr. Lydia Heck for her assistance in this context.

[1] J. Tennyson and J. R. Henderson, J. Chem. Phys. **91**, 3815 (1989).
[2] O. Brass, J. Tennyson, and E. Pollak, J. Chem. Phys. **92**, 3377 (1990).
[3] J. R. Henderson and J. Tennyson, Chem. Phys. Lett. **173**, 133 (1990).
[4] C. R. Le Sueur, J. R. Henderson, and J. Tennyson, Chem. Phys. Lett. **206**, 429 (1993).
[5] G. Garćia de Polavieja, N. Fulton, and J. Tennyson, Mol. Phys. **83**, 361 (1994).
[6] D. A. Sadovski, N. G. Fulton, J. R. Henderson, J. Tennyson, and B. I. Zhilinskií, J. Chem. Phys. **99**, 906 (1993).
[7] J. R. Henderson and J. Tennyson, Mol. Phys. **69**, 639 (1990).
[8] J. R. Henderson, H. A. Lam, and J. Tennyson, J. Chem. Soc., Faraday Trans. **88**, 3287 (1992).
[9] D. M. Leitner, J. D. Doll, and R. M. Whitenell, J. Chem. Phys. **94**, 6644 (1994).
[10] C. Chakravarty, R. J. Hinde, D. M. Leitner, and D. J. Wales, Phys. Rev. E **56**, 363 (1997).
[11] N. J. Wright and J. M. Hutson, J. Chem. Phys. **110**, 902 (1999).
[12] J. M. Gomez Llorente and E. Pollak, J. Chem. Phys. **90**, 5406 (1989).
[13] A. Carrington and R. A. Kennedy, J. Chem. Phys. **81**, 91 (1984).
[14] R. Guantes, A. Nezis, and S. C. Farantos, J. Chem. Phys. **111**, 10836 (1999).
[15] J. Tennyson, O. Brass, and E. Pollak, J. Chem. Phys. **92**, 3005 (1990).
[16] J. Higgins, W. E. Ernst, C. Callegari, J. Reho, K. K. Lehmann, G. Scoles, and M. Gutowski, Phys. Rev. Lett. **77**, 4532 (1996).
[17] J. Higgins, T. Hollebeek, J. Reho, T.-S. Ho, K. K. Lehmann, H. Rabitz, and G. Scoles, J. Chem. Phys. (to be published).
[18] J. C. Light, I. P. Hamilton, and J. V. Lill, J. Chem. Phys. **82**, 1400 (1985).
[19] Z. Bačić and J. C. Light, Annu. Rev. Phys. Chem. **40**, 469 (1989).
[20] S. E. Choi and J. C. Light, J. Chem. Phys. **92**, 2129 (1990).
[21] D. O. Harris, G. G. Engerholm, and W. D. Gwinn, J. Chem. Phys. **43**, 1515 (1965).
[22] D. C. Sorensen, SIAM J. Matrix Anal. Appl. **13**, 357 (1992).
[23] R. B. Lehoucq, K. Maschoff, D. C. Sorensen, and C. Yang, ARPACK, available from ftp://ftp.caam.rice.edu/pub/software/ARPACK.
[24] P. P. Korambath, X. T. Wu, and E. F. Hayes, J. Phys. Chem. **100**, 6116 (1996).
[25] T.-S. Ho and H. Rabitz, J. Chem. Phys. **104**, 2584 (1996).
[26] M. Gutowski, J. Chem. Phys. **110**, 4695 (1999).
[27] S. Wolf, G. Sommerer, S. Rutz, E. Schreiber, T. Leisner, and L. Wöste, Phys. Rev. Lett. **74**, 4177 (1995).
[28] D. W. Boo, Y. Ozaki, L. H. Anderson, and W. C. Lineberger, J. Phys. Chem. A **101**, 6688 (1997).
[29] T. Leisner, S. Vajda, S. Wolf, L. Wöste, and R. S. Berry, J. Chem. Phys. **111**, 1017 (1999).